Instrumentation and machine protection strategy for the ESS target station

T J Shea[1], L Coney[1], R Linander[1], A Jansson[1], E Pitcher[1], A Nordt[1], C Thomas[1], H D Thomsen[2]

[1] European Spallation Source, P.O Box 176, SE-221 00 Lund, Sweden
[2] ISA - Centre for Storage Ring Facilities, Aarhus University, DK-8000 Aarhus, Denmark

E-mail: thomas.shea@esss.se

Abstract. The European Spallation Source (ESS) linear accelerator will deliver a 5 MW, low-emittance 2 GeV proton beam directly to the target station at a rate of 14 Hz. The target is composed of helium-cooled plates of tungsten housed within a rotating wheel 2.5 meters in diameter. To limit power density, a transport line expands the proton beam to centimeter scale and rasters the expanded beam across the target surface. This technique produces a reasonably uniform current density that allows a service life of five years for the rotating tungsten target and six months for the upstream proton beam window. Conversely, the low emittance of the beam allows an errant spot size small enough to damage target station components within a single 2.86 millisecond pulse. A suite of instrumentation systems located within the target monolith and further upstream in the transport line will detect errant conditions in both the beam and target. Instrumentation dedicated to monitoring target properties such as helium coolant flow, target balance and motion will be located on the downstream side of the target away from the incoming proton beam. Proton beam density, position, current, and halo properties will be monitored upstream of the target. Precise synchronization of the beam pulse and target rotation will also be done using beam arrival measurements. Detection of errant conditions will trigger the suppression of beam production via the Beam Interlock System within the ESS Machine Protection System. This paper will introduce the primary causes of damaging beam properties and describe the measurement techniques that will detect them on a time scale sufficiently fast to mitigate component damage.

1. Introduction

The ESS facility will integrate a 5 MW target station with a proton linear accelerator that produces 2.86 ms long pulses of 2 GeV protons. At full power, each pulse has a peak current of 62.5 mA and occurs at a repetition rate of 14 Hz. Beam transport from the accelerator to the target is depicted in figure 1. Upon inspection, the two distinct regions become apparent: the accelerator region upstream of the beam waist (marked CO in the figure), and the target region downstream of the waist. They are separated by a 2 m thick neutron shield wall that surrounds the beam waist and isolates the accelerator from the target. The two regions also have two unique rulebooks. In the accelerator, the design is driven by the requirement to accelerate and transport the beam with a loss of less than 1 W/m. This low loss requires a very low emittance beam inside of a relatively large aperture, and results in low activation that allows hands-on maintenance. Downstream, the target station must absorb both this primary beam and also the unmoderated spallation products. This requires a dramatically expanded beam

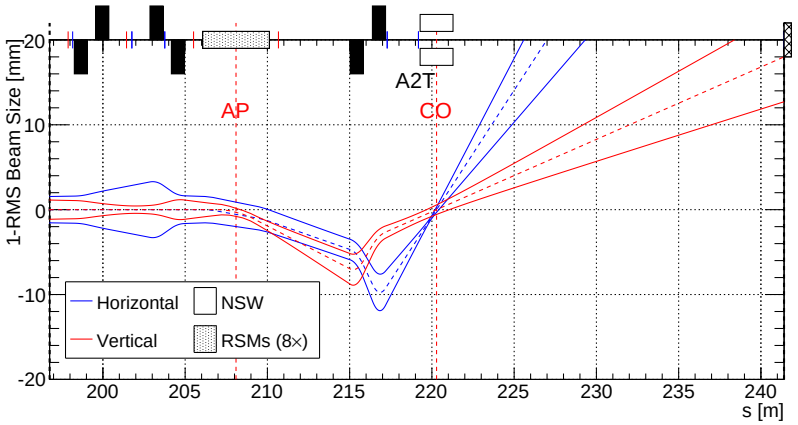

Figure 1: The 1-RMS transverse beam sizes along the beam delivery line from the accelerator to the target (far right edge of plot) at maximum raster amplitudes. The location and polarity of 6 DC quadrupoles are represented by black boxes.

passing through the target monolith's relatively tight shielded aperture. Here, maintenance is performed by remote handling.

The accelerator-to-target (A2T) line on the left side of figure 1 acts as the beam delivery system, transforming the small, bright proton beam from the ESS linac into a beam acceptable for the target components. Table 1 lists the primary parameters of the beam at the target and at the proton beam window (PBW) located about 4 meters upstream of the target. Within the target station, cooling systems and features like the rotating target wheel allow it to accept the full 5 MW beam. To achieve a neutron production run of several months between major maintenance periods, the beam delivery and target systems must all function correctly. With many target components operating near their engineering limits, instrumentation must detect target system malfunctions and errant beam conditions before damage occurs, and the machine protection system must promptly suppress proton beam production.

2. Beam Delivery

The A2T line must meet several requirements:

- Match the linac beam to the macroscopic beam size required at the target.
- Keep the beam tails contained while defocusing the beam at the target.
- Reduce the local time-averaged beam intensity at the Proton Beam Window (PBW) and target.
- Facilitate a Neutron Shield Wall (NSW) that allows efficient transmission of the primary beam but but presents a narrow aperture to the neutrons backstreaming from the target. All magnets should preferably be located upstream of this wall.

The requirements above are met by a transverse beam raster system that relies on a combination of DC and fast AC magnetic elements to moderately expand the linac beam and sweep it rapidly across the target.

2.1. The AC Optics

As described in [1, 2], the ESS will incorporate a raster system that sweeps the accelerator beamlet in a transverse pattern across the target surface. This technique lowers the time-averaged beam intensity while containing the beam within a defined rectangular footprint. A

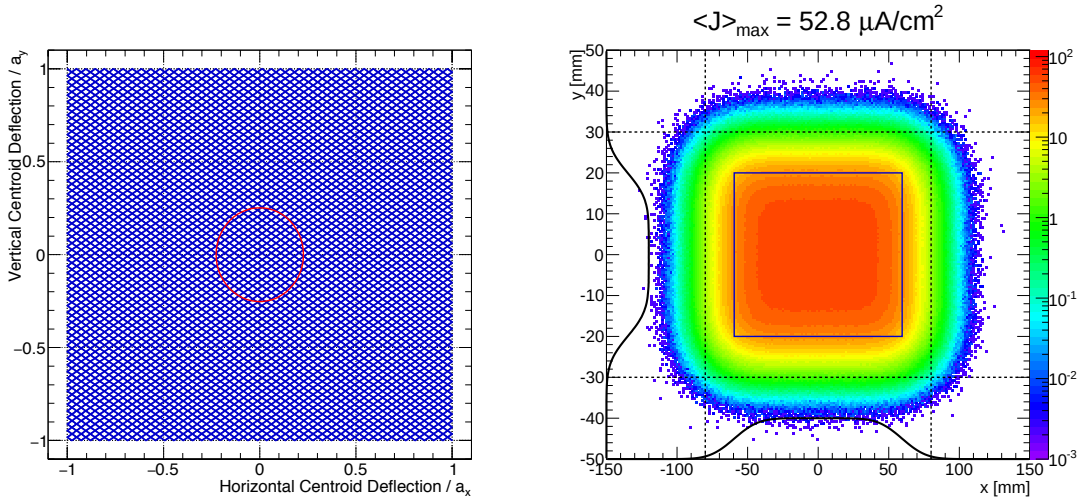

(a) A Lissajous-pattern generated by triangle waveforms with a frequency ratio of 113/83. For comparison, the beamlet relative RMS sizes at the BEW are illustrated by a red ellipse.

(b) The intensity distribution is scaled to represent the peak current density, normalized to 2.5 mA average current. The blue rectangle illustrates the outline of the raster pattern. The dashed lines indicate the footprint containing 99.0% of the beam.

Figure 2: Simulated raster pattern and consequent intensity distribution at the target BEW following a full cycle of the Lissajous-pattern with the beam parameters in Table 1.

2D mesh of interwoven sweep trajectories is generated through a Lissajous-like pattern. Such a pattern is defined by a frequency ratio f_x/f_y and phase ϕ_{xy} of two non-harmonic triangular sweep waveforms. The waveforms are applied to two sets of AC raster scanning magnets (RSMs) operating in the two transverse directions. By choosing very non-harmonic raster frequencies, e.g. $f_x/f_y = 113/83$, the patterns can reach almost limitless complexity, cf. figure 2a. The resulting sweep pattern will of course be convoluted with the beamlet profile. The uniformity of the resulting distribution will depend on the spacing between the respective sweeps relative to the beamlet size. A fine mesh would also to a large extent smear the beam profile, thus leaving the effective distribution more insensitive to the details of the beamlet profile.

To introduce the necessary oscillating beam displacements near the target, the raster system is foreseen to consist of 8 colinear raster scanning magnets (RSMs), two sets of 4 acting in the respective transverse planes. The RSMs in a set should ideally be synchronized and share the same field amplitude, but each of the 4 in a set are independent modules, thus eliminating some single points of failure. To avoid the need for active cooling of magnets and power supplies, the raster system is foreseen to be operated at a duty cycle of only 5%, appropriately more than the 4% beam pulse duty cycle (2.86 ms at 14 Hz).

2.2. The DC Optics

To facilitate a small-aperture Neutron Shield Wall (NSW), the DC optics provides more than the means to set the size of the beamlet that is rastered across the target. By design, the AC displacements neutralize at a crossover point (CO) between the final magnetic elements and the target. By also setting a very small beam size at the CO, this is an ideal location for the NSW. This scheme requires a minimum of 6 DC quadrupoles. The location of the DC quadrupoles and 8 RSMs can be inspected in figure 1.

The final quadrupole doublet, downstream of the RSMs, neutralizes the raster displacements

Table 1: Beam parameters, horizontal (H) and vertical (V).

Parameter	Unit	Location	H	V
RMS beam size	mm	CO	0.14	0.64
	mm	PBW	10.7	4.10
	mm	target	13.5	5.05
Max. displacement	mm	PBW	47.1	15.8
(rastering)	mm	target	59.5	20.0
f_w	kHz	—	39.55	29.05
Avg. current density	μA/cm^2	PBW	84	
	μA/cm^2	target	53	
Footprint: 99.0%	mm	target	160	60
99.9%	mm	target	180	64

at the CO by imposing a transverse phase advance of 180° between the common raster magnet action point (AP) and the CO. Assuming the nominal optics, the CO thus becomes a pivot point of the oscillating raster motion. The first 4 quadrupoles of the A2T constitute a matching section that provides a minimum beam size at the CO while setting the $\simeq$ cm^2 beamlet size on the target. Assuming the parameters of table 1, a simulation of the intensity distribution at the target following each 2.86 ms beam pulse is shown in figure 2b. The distribution contains a relatively large uniform central region and respects the marked footprint, enclosing $\geq 99.0\%$ of the beam.

A snapshot of the beam optics, while the raster actions are at maximum amplitudes, is visible in figure 1. It is quite clear that the displacements are considerable compared to the 1-RMS beam sizes, especially downstream of the CO. Apart from providing the CO condition, the final quadrupole doublet also magnifies the angular deflection in the horizontal plane, thus balancing the amplitude setpoint of the RSMs acting in the two directions despite the $\simeq 3:1$ amplitude ratio required, cf. table 1.

3. Instrumentation

Three classes of instrumentation will be deployed to detect errant conditions:

(i) Beam delivery system instrumentation.

(ii) Target system instrumentation

(iii) Proton beam instrumentation

Subsection 3.1 briefly describes the instrumentation that will monitor the beam delivery magnets. In subsections 3.2 and 3.3, target and proton beam instrumentation receive a more detailed treatment. All of these systems can interface to the machine protection system (described in Section 4) in order to suppress beam production upon detection of errant conditions.

3.1. Beam Delivery System Instrumentation

Instrumentation will monitor the AC and DC magnet systems that determine the beam delivery optics. Being critical components, each raster scanning magnet will contain a Bdot loop which will directly monitor the derivative of the triangular magnetic field waveform. Under nominal

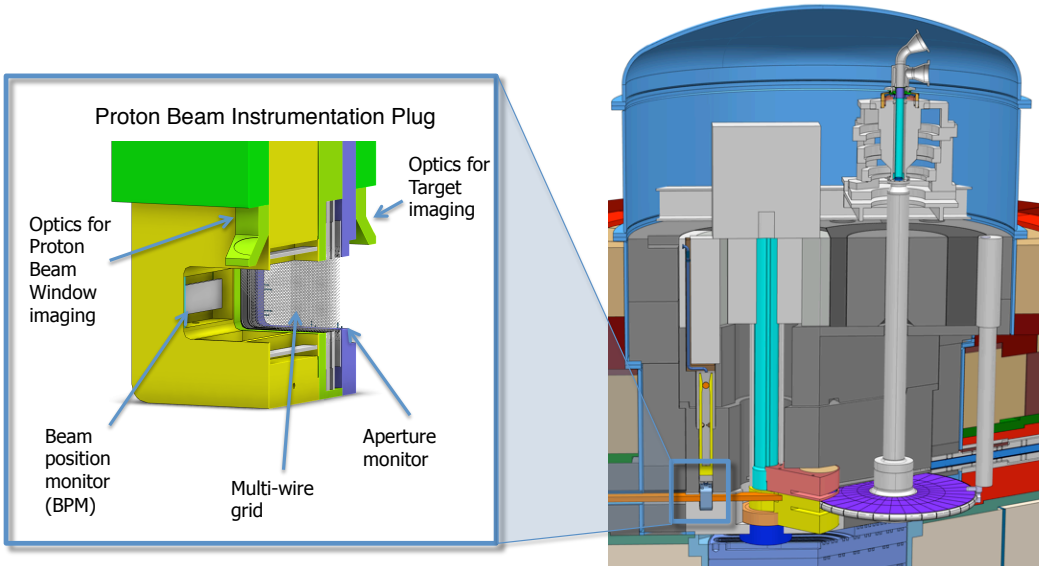

Figure 3: Conceptual rendering of the target monolith. Incoming proton beam (orange) from the left passes though the proton beam window (not shown), then through the proton beam instrumentation plug (gray) and between the upper and lower moderator plugs (brown and yellow) before reaching the target wheel (purple). The wheel shaft (gray) extends approximately 5 m up to the drive and bearing unit, which also contains the pipe connections to the target primary cooling system. The target monitoring plug (gray) is located downstream of the target wheel. The inset on the left depicts the devices contained in the proton beam instrumentation plug.

conditions, the observed signal is a square waveform that occurs during the entire 2.86 ms duration of the beam pulse. Each of the raster magnets will be monitored independently. The current and voltage of the DC magnet circuits will be monitored and a window comparator will be used to detect deviation from the nominal set points. The monitored and interlocked magnets include all eight raster scanning magnets, the six quadrupoles, and four 2D dipole correctors.

3.2. Target System Instrumentation

The ESS target is a volume of tungsten contained in a wheel-like steel structure, cf. figure 3, that is rotating to spread the heat deposition and radiation damage. It is continuously cooled by pressurized helium circulated through a long shaft. On top of the shaft there is a drive and bearing unit that rotates the target wheel synchronized with the impinging pulsed proton beam. The integrity and lifetime of the target wheel as well as sufficient reliability and availability of the drive and bearing system is depends on maintaining the operating conditions within specified ranges. Pressure and temperature surges, vibrations, deficient cooling flow, and misalignment may lead to failure or unavailability of the system. Therefore, extensive instrumentation will be deployed to monitor the performance and condition of the wheel and give relevant input to the machine protection system. Additional instrumentation will monitor other major components within the target station and with moderate response time, could detect the impact of persistent errant beams.

3.2.1. Target wheel rotation and helium coolant flow The two most important parameters assure are the stable and precise rotation of the wheel and a sufficient mass flow of the helium coolant. Failure to maintain these conditions may lead to overheating of the wheel with

subsequent structural damage or lifetime reduction.

The rotation of the wheel, nominally 25.5 RPM, will be monitored by instrumentation located on the target drive unit. Rotary encoders and magneto resistive sensors are envisaged to be mounted on the motor unit and the target wheel shaft. Other means of measuring the wheel rotation, if redundancy is required, may utilize the optical path to the target wheel disc that the target monitoring plug provides. This target monitoring plug is located downstream of the wheel.

The nominal mass flow of the helium coolant is set to 3 kg/s with an inlet temperature of approximately 40 degrees celsius. The cooling system will be equipped with several sensors for monitoring the helium flow rate, inlet and outlet temperature, pressure level and other important process parameters. Some of those measurement points will be dedicated to machine protection.

3.2.2. Condition monitoring of the target wheel unit In order to achieve expected availability and reliability for the target wheel unit, it is essential to understand condition of the system and its individual parts. Early indications when operating parameters begin to divert from their normal values are needed for good planning of preventive maintenance. Flow rate, pressure and temperature measurements in the primary target cooling system will be monitored and recorded in order to discover deviations from normal operating conditions. That system is also proposed to contain a radioisotope sampling for early detection of unexpected release of volatile isotopes that could indicate damage of the spallation material.

The target wheel unit will, in addition to sensors measuring the rotation, be equipped with vibration and balance monitors as well as conventional motor and bearing condition monitors. For example, it is important to keep track of the degradation trends of bearings in order to plan for replacement at the right time.

The target monitoring plug, located downstream of the target wheel, will provide the possibility to use techniques like Laser Doppler Vibrometer, infrared temperature measurement and visible imaging for detection of vibrations, wobbling, mechanical misalignment, deformations, and thermal hotspots.

3.3. Proton Beam Instrumentation

In the target monolith and upstream, a suite of instrumentation will characterise the proton beam delivered to the target. This suite is based on concepts presented in [4]. The measurements will include the beam current, beamlet position, beam current density distribution, and the beam halo approaching the aperture.

3.3.1. Beam Current Monitors The beam current will be measured in A2T by two redundant Beam Current Monitor (BCM) systems based on the AC Current Transformers [3]. After digital filtering, these devices will provide a time resolution of about 1 μs and an amplitude precision of about 1 mA. In the context of target protection, these systems provide several indirect functions. The BCM data helps to verify that the peak current and the average power are within the operating envelope approved for the target station. Imaging and grid systems normalize their data to BCM measurements so that intensity and fluence on target components can be accurately determined. Finally, the BCM provides pulse time-of-arrival information to support synchronization of the rotating target wheel.

3.3.2. Target Beam Position Monitor In addition to several traditional beam position monitors (BPM) in the A2T line, a BPM in the target monolith will monitor the beamlet position as it moves transversely during the pulse. The speed of this transverse motion exceeds 10 mm/μs and the position monitor must measure with a precision of a few mm. Therefore, the sample rate will exceed 1 MSa/s.

The beamline device will consist of electrodes as well as radiation tolerant coaxial cables and feedthroughs that bring the 352 MHz signals to the exterior of the monolith, where the signals will be processed. As depicted by figure 3, this electrode resides within the proton beam instrumentation plug. The aperture exceeds 200 mm horizontally, and thus considerable design effort will have to be expended to optimize performance. In particular, the signal to noise ratio at the 352 MHz bunching frequency will have to be high enough to ensure millimeter resolution over an approximate 1 MHz bandwidth, even with bunches that have lengthened during their >200 m drift from the linac.

The BPM electronics will first measure the position of the beamlet versus time within the pulse. To provide the interlock function, these measurements can be compared to reference waveforms. With further processing and an assumed beamlet size, an estimated map of the current density or other figures of merit can be synthesised and directly compared with the target requirements. The system will detect errant conditions within the pulse.

3.3.3. Imaging Systems Two imaging systems will measure the 2D current density at the proton beam window and at the surface of the target wheel. They will measure variations of the peak density to a precision of about 10% with a spatial resolution of about 1 mm. Position of the centroid will also be determined with a precision of about 1 mm. To achieve this performance, the systems will average over an entire pulse.

Figure 3 shows the location of the first mirrors, with one looking upstream at the proton beam window and one looking downstream at the target. The primary components of the reflective optical systems reside within the proton beam instrumentation plug. The images are transported to the top of the monolith and then out to an area hospitable to cameras and other electronics. The source of these images is light produced as the protons pass through luminescent coatings on the window and target. Although it possesses a luminescent lifetime of a few ms, a coating of thermal-sprayed alumina doped with Chromium meets the requirement to measure individual pulses. Other technologies will be explored with the goal of providing intra-pulse measurements.

3.3.4. Grid System The grid system will consist of one multiwire grid assembly located in the target monolith. Two locations are under consideration: in the Proton Beam Window assembly and in the proton beam instrumentation plug. In the first location, the grid assembly would be located in vacuum just upstream of the window, while in the second location, depicted in figure 3, the grid assembly will be immersed in Helium at about atmospheric pressure. The device will measure the horizontal and vertical projections of the beam current density such that changes of 20 percent with respect to nominal peak density can be accurately determined. The grid's wire spacing is driven by the spatial resolution requirement of a few mm in either dimension, leading to a density of about a few wires per cm. The system will be interfaced to the beam interlock system so that beam can be interrupted within the pulse if the current density exceeds a programmable threshold. The goal is to make this determination in less than 100 μs.

3.3.5. Aperture Monitors Aperture monitors consist of fixed sensors surrounding the apertures of the proton beam window and the proton beam instrumentation plug. In addition, moveable sensors will reside close to the upstream aperture of the neutron shield wall. The fixed units in the monolith will ensuring that less than 0.1% of the total beam current resides outside the defined footprint. Sensors on the moveable unit will be set far outside of the beam core, but close enough to detect the result of deviations from nominal DC optics.

The baseline concept for the sensor is a thermocouple array that can detect errant conditions after many pulses. To achieve faster response, a complementary technique that measures current induced by the charged particle shower will also be deployed. At the shield wall, the background

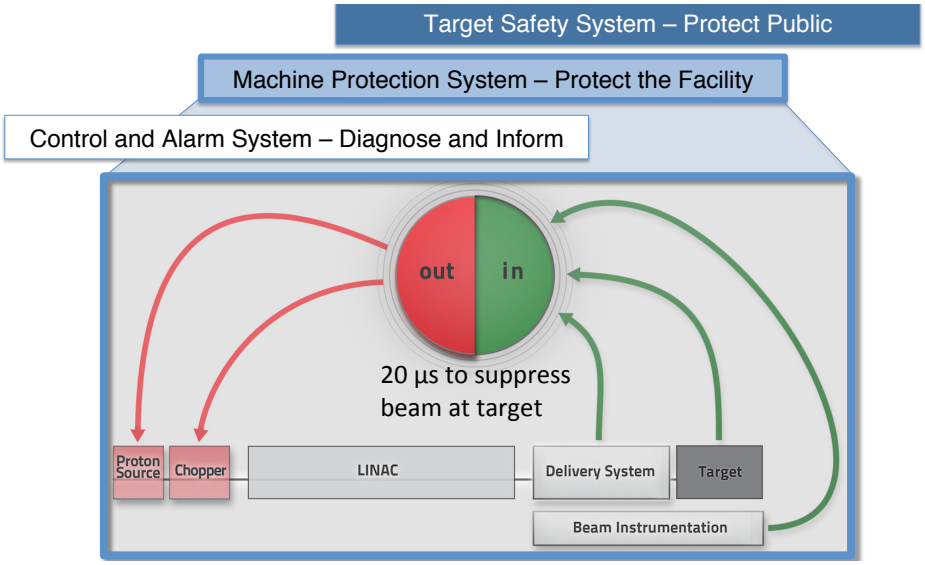

Figure 4: Overview of of the Machine Protection System

should be low enough to enable the additional method of direct shower detection. Measurements within the pulse should be achievable.

4. Machine Protection System

Figure 4 shows the three layers of protection applied to the ESS target station. At the lowest integrity level, the control system provides a rich set of diagnostic data to operators. A subset of this data can trigger alarms, in many cases allowing operators to make corrections before the machine protection system trips. At the top of the figure, the target safety system provides the highest integrity level but only interrupts beam production under the most dire circumstances for the purpose of protecting the public. The machine protection system occupies the middle layer, providing an integrity level consistent with its mission of protecting hardware components for the purpose of achieving the availability goals of the ESS facility [5].

The lower portion of figure 4 shows the signal flow of the beam interlock system as it relates to target protection. Here, signals from the three types of instrumentation described above (green in the figure) reach back to two devices (red in the figure) to suppress beam production. After the errant condition is detected near the target station, the signal propagates thought the interlock system, first interrupting the beam pulse with the transverse chopper at 3.5 MeV, and also stopping the rest of the pulse with slower devices upstream. About 4 μs of beam remains in the accelerator and this is still delivered to the target area. The total time from detection to the last proton arriving at the target is under 20 μs . The errant conditions that can cause this to occur are described in the next section.

5. Errant Conditions

Before permitting beam on target, the instrumentation described in Sections 3.1 and 3.2 must collectively indicate that the beam delivery system and the target station are ready for the intended operational mode. This mode defines the allowed equipment state and the envelope of beam parameters, from the very restrictive set that may be use for low power verification up to the full pulse length, peak current, and repetition rate of 5 MW operations. During operations, this instrumentation suite can interrupt production upon detection of an equipment

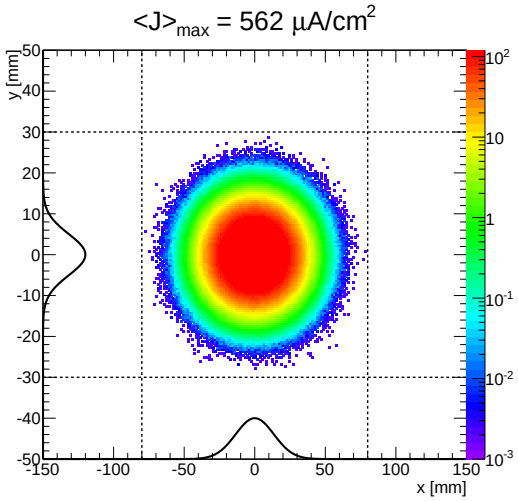

(a) Full raster system failure: unrastered beamlet.

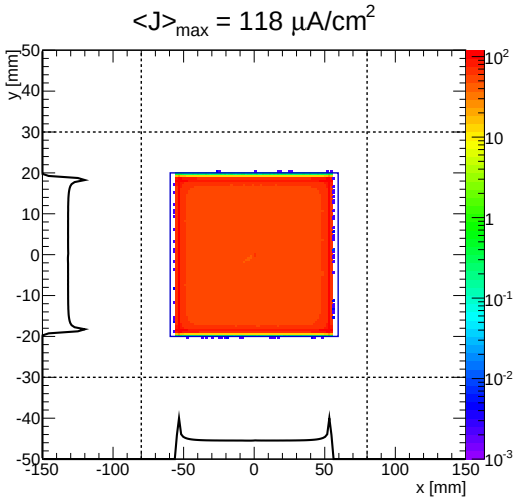

(b) Beamlet size decrease: a RMS size of 0.3 mm is assumed in both transverse directions.

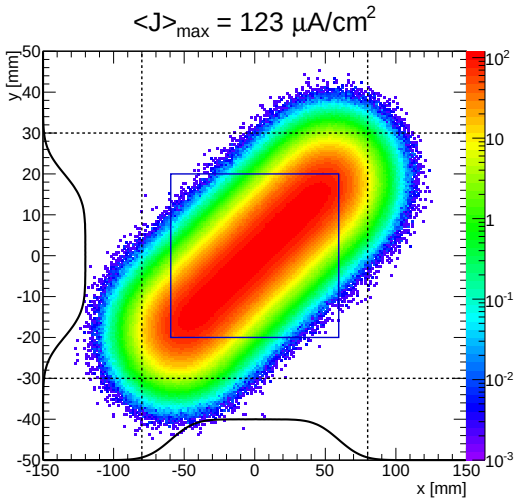

(c) Raster pattern reduction: $f_x/f_y = 1$.

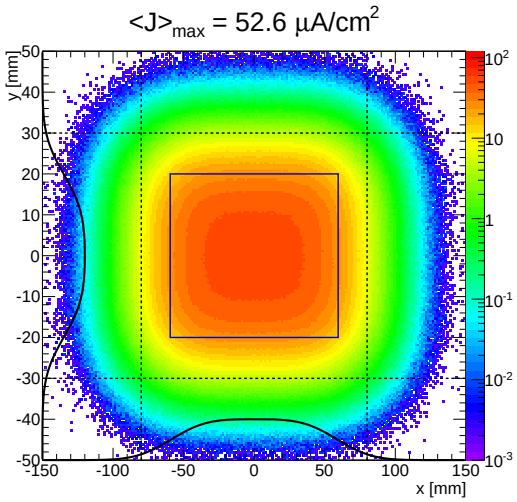

(d) Beamlet size increase: a 50% increase in RMS sizes is assumed.

Figure 5: Simulations similar to Fig. 2b but including failures.

state inconsistent with the operational mode.

Having described the intended operation of the A2T line, it is evident that several conditions need to be met in order to deliver the nominal beam to the target. Any upstream quadrupole failing to deliver the intended integrated gradient will affect the beamlet size on the target. Due to the raster approach, the time-averaged beam distribution is fairly insensitive to such a change. Contrarily, if the final doublet is not performing as intended, the beam centroids will oscillate at the CO and the beamlet size and raster pattern will be affected at the target. These cases, and the examples that follow should first be detected by beam delivery instrumentation. Should this fail, the beam instrumentation will detect the result of the delivery system problem (errant beam parameters), and if that fails, then a subset of target instrumentation might detect the result of the persisting errant beam (usually power deposition where it should not be).

Figure 5 shows a few examples of how the time-averaged beam distribution responds to

Table 2: Errant beam conditions

Event	Cause	Unmitigated Effect	Detection
RSM full failure, $\times 1$	Power supply failure, misconfiguration	$J_{\max}$ increases by $\times 1.33$	Intra-pulse: BPM, grid, Bdot; Avg: imaging
RSM full failure, $\times 8$	As above, RSM and beam pulse synchronization	$J_{\max}$ increases by $\times 10$	As above, but BCM with Bdot
Beam on target is displaced	DC correctors, misaligned input beam, misconfiguration	Beam losses along the monolith beam duct	Intra-pulse: BPM, aperture; Avg: imaging, target
Beamlet size on target too small	Quadrupole failure (power supply, misconfiguration)	Intensity edges and peaks in beam distribution, $\simeq \times 2$	Intra-pulse: grid, aperture(NSW); Avg: imaging
Final quad. doublet failure	Power supply failure, misconfiguration	Beamlet misfocused, raster ampl. changes	Intra-pulse: BPMs, grid, aperture; Avg: target, imaging
Beam energy deficiency	RF errors or cavity trips	As above, vertical displacement	As above
Raster pattern reduction	Misconfiguration	Intensity increase: footprint not exploited	Intra-pulse: BPM, grid; Avg: imaging

failures to provide the proper beamlet and raster system parameters. Table 2 contains a list of selected failure events and how they will be detected, both within the pulse (Intra-pulse) and after averaging over one or more pulses (Avg.).

Compared to the unrastered beamlet, the raster system reduces the time-averaged peak current density by more than an order of magnitude. A complete raster system failure, shown in figure 5a, is thus believed to be the most detrimental single error. Since the RSM system and beam are pulsed, this failure could originate not only from configuration or hardware issues in the RSM system, but also from a desynchronization of the pulsed beam and RSM system. Total failure would first be detected by the Bdot probes alone. Bdot signals combined with BCM readings would catch the desynchronization case. In the target station, the BPM and grid would detect the unrastered beam within the pulse, while the imaging systems would detect the density increase after the pulse completes. In this example, as in most, the target instrumentation would probably not play a role unless the condition persisted long enough to cause damage.

The rastered distribution could benefit (in terms of reduced peak intensity and sharper edge) from reducing the beamlet dimensions. This would however increase the static beamlet power density, which might damage the PBW or the target wheel within one pulse in case of full failure of all 8 RSMs. Figure 5b shows the result of delivering the smallest beamlet size realistically producible. With the smaller beamlet dimensions, high-intensity edges and corner peaks become severely pronounced as a result of the finite raster waveform bandwidth, *i.e.* turning time. As long as the RSM system is operational, the local intensity would increase by a factor $\simeq 2$. It is unlikely to minimize the beamlet dimensions on target without simultaneously increasing the beam size considerably in the upstream quadrupoles. Therefore, movable aperture monitors should be able to detect such an error. In addition, the grid and the imaging systems could

directly observe any significant local density increases.

The complex Lissajous-like raster pattern is easily generated by maintaining a close-to-irrational ratio of raster frequencies. This pattern can be severely reduced in complexity if f_x/f_y unintentionally changes and approaches an integer. Figure 5c depicts the worst case where $f_x/f_y = 1$, possibly due to a configuration error, resulting in a single diagonal raster line. Again, the failure leads to a local intensity increase by a factor $\simeq 2$. Since a configuration error is the most likely cause, the delivery system instrumentation would not catch the issue, and detection would depend upon the collection of beam instrumentation devices that observed example 5a.

In the final failure mode example, shown in figure 5d, the beamlet dimensions are 50% larger than the respective nominal values. The peak intensity of the rastered distribution is not affected significantly, but the beam tails leak outside the nominal footprint regions. During the pulse, the aperture monitors would provide the most sensitivity to this condition, followed by the grid. The imaging systems may detect it after a single pulse, and much later, the target instrumentation may detect elevated temperatures in some components near the aperture.

6. Outlook

As the design of the ESS target station and A2T transport line proceeds, development of the machine protection strategy will continue in parallel. A number of events that could cause errant beams have already been considered and this has informed the design of the relevant instrumentation systems. Many more cases remain to be analyzed, including some more insidious than those presented here, and this analysis will result in further refinement of the instrumentation suite. Although the harsh environment of the target station presents a major challenge to the design of reliable instrumentation, the planned redundant and diverse systems should provide appropriate inputs to the beam interlock system, and therefore help to achieve the performance goals of the ESS facility.

References

[1] Thomsen H D Holm A Møller S P *et al.* 2013 A linear beam raster system for the European Spallation Source? *Proc. International Particle Accelerator Conference* (Shanghai)

[2] Thomsen H D and Møller S P 2014 The ESS high energy beam transport after the 2013 design update *Proc. International Particle Accelerator Conference* (Dresden)

[3] Hassanzadegan H Jansson A Thomas C Legat U Strnisa K Crisp J and Werner M 2014 Design, implementation and preliminary test results of the ESS beam current monitor system *Proc. International Particle Accelerator Conference* (Dresden)

[4] Shea T Böhme C Cheymol B Gallimore S Hassanzadegan H Pitcher E, and Thomsen H D 2013 Proton beam measurement strategy for the 5 MW European Spallation Source Target *Proc. International Beam Instrumentation Conference* (Oxford)

[5] Nordt A Apollonio A and Schmidt R 2014 Overview on the design of the machine protection system for ESS *Proc. International Particle Accelerator Conference* (Dresden)